PERGAMON

Computers in Biology and Medicine 31 (2001) 429–440

Computers in Biology and Medicine

www.elsevier.com/locate/compbiomed

# Electroencephalogram analysis using fast wavelet transform

Zhong Zhang[a,*], Hiroaki Kawabata[b], Zhi-Qiang Liu[c]

[a] *Department of System Engineering, Industrial Technology Center of Okayama Prefecture 5301 Haga, Okayama 701-1296, Japan*

[b] *Faculty of Computer Science and System Engineering, Okayama Prefecture University 111 Kuboki, Soja 719-1197, Japan*

[c] *Department of Computer Science & Software Engineering, The University of Melbourne, Vic., 3010, Australia*

Received 30 October 2000

**Abstract**

The continuous wavelet transform is a new approach to the problem of time–frequency analysis of signals such as electroencephalogram (EEG) and is a promising method for EEG analysis. However, it requires a convolution integral in the time domain, so the amount of computation is enormous. In this paper, we propose a *fast wavelet transform* (FWT) that the corrected basic fast algorithm (CBFA) and the fast wavelet transform for high accuracy (FWTH). As a result, our fast wavelet transform can achieve high computation speed and at the same time to improve the computational accuracy. The CBFA uses the mother wavelets whose frequencies are 2 octaves lower than the Nyquist frequency in the basic fast algorithm. The FWT for high accuracy is realized by using upsampling based on a L-Spline interpolation. The experimental results demonstrate advantages of our approach and show its effectiveness for EEG analysis. 

*Keywords:* Wavelet transform; Fast algorithm; EEG analysis; Computation speed; Computation accuracy

## 1. Introduction

The Electroencephalogram (EEG) is a resultant signal of the active potentials of many nerve cells in the cerebral cortex, and captures the cerebral function. EEG is one of the irregular and feeble signals in the living body. Researchers have investigated effective analysis methods for many years. In recent years, the wavelet transform has been used for the analysis of EEG signals, and has been effective in the elucidation of sleep apnea syndrome, epilepsy, etc. [1,2].

* Corresponding author. Tel.: +81-86-286-9620; fax: +81-86-286-9630.
*E-mail address:* zhang@okakogi.go.jp (Z. Zhang).

0010-4825/01/$ - see front matter 
PII: S0010-4825(01)00019-1

A continuous wavelet transform (WT) maps a time function into a two-dimensional function of $a$ and $b$, where $a$ is the scale ($1/a$ denotes frequency) and $b$ is the time translation [3]. For a signal $x(t)$, the WT can be written as follows:

$$w(a,b) = a^{-1/2} \int_{-\infty}^{\infty} x(t)\bar{\psi}\left(\frac{t-b}{a}\right) \mathrm{d}t, \tag{1}$$

where $\psi(t)$ is a mother wavelet (MW), $\bar{\psi}_{a,b}(t)$ denotes the complex conjugate of $\psi_{a,b}(t)$, and $\psi_{a,b}(t)$ stands for a wavelet basis function.

The MW $\psi(t)$ is an oscillatory function whose Fourier transform $\hat{\psi}(\omega)$ must satisfy the following admissibility condition:

$$C_\psi = \int_{-\infty}^{\infty} \frac{|\hat{\psi}(\omega)|^2}{|\omega|} \mathrm{d}\omega < \infty. \tag{2}$$

If this condition is satisfied, $\psi(t)$ has zero mean, and the original signal can be recovered from its transform $W(a,b)$ by the inverse transform

$$x(t) = \frac{1}{C_\psi} \int_{-\infty}^{\infty} \int_{-\infty}^{\infty} W(a,b) a^{-1/2} \psi\left(\frac{t-b}{a}\right) \frac{\mathrm{d}a\,\mathrm{d}b}{a^2}. \tag{3}$$

As shown in Eqs. (1) and (3), the WT is a convolution integral in the time domain, so the amount of computation is enormous and it is impossible to analyze EEG signals in real time. Over the last two decades, researchers have proposed some fast wavelet transform algorithms [4]. Traditionally, the á-trous algorithm [5] and the fast algorithm in the frequency domain [6] are used. The latter is used more for computation speed [7] and has the following properties: (1) It uses multiplication in the frequency domain instead of convolution in the time domain; (2) It uses one octave of the mother wavelet to obtain other mother wavelets for all octaves by down-sampling based on the self-similarity of the mother wavelet. However, this algorithm has some major problems, in particular, the computational accuracy is lower than the usual WT and it is difficult to satisfy the accuracy requirement of analysis for EEG.

In this paper, we propose a fast wavelet transform (FWT) which includes the corrected basic fast algorithm and fast wavelet transform for high accuracy (FWTH) that improves the accuracy at a high computational speed. We will examine the characteristics of the FWT using a model signal and demonstrate its effectiveness in EEG analysis.

## 2. Fast wavelet transform

### 2.1. Basic algorithm of WT

Parameters $a$ and $b$ in Eq. (1) take a continuous value; however, for computational purposes, they must be digitized. Generally, when the basic scale is set to $\alpha = 2$, then $a_j = \alpha^j = 2^j$ is called octave $j$. For example, the Nyquist frequency $f_N$ of the signal corresponds to the scale $a_0 = 2^0 = 1$, and the frequency $f_N/2$ corresponds to $2^1$ and is referred to as 1 octave below $f_N$, or simply octave one. As for the division of the octave, we follow the method of Rioulmay [8] and divide the octave into $M$ divisions ($M$ voices per octave) and compute the scale as follows:

$$a_m = 2^{i/M} 2^j, \tag{4}$$

where $i=\{0,1,\ldots,M-1\}$, $j=\{1,\ldots,N\}$, $N$ is number of the octave, $m=i+jM$. $b$ is digitized by setting $b=k\Delta t$, where $\Delta t$ denotes sampling interval.

As shown in Eq. (4), the scale $a_m$ is $2^{i/M}$ times $2^j$, which expresses that the MW has the self-similarity property and the MW of the scale $a_m$ can be calculated from the MW of the scale $2^{i/M}$ by down sampling $2^j$. In this paper, therefore, we first prepare the $\psi_i(n)\,(i=0,1,\ldots,M-1)$ for one octave from the maximum scale (the minimum analysis frequency) of analysis which corresponds to scale $2^N 2^{-i/M}$:

$$\psi_i(n)=2^{-N/2+i/2M}\psi(2^{-N+i/M}n) \tag{5}$$

and then calculate $\psi_m(n)$ by a sampling of the $2^{N-j}$ twice of $\psi_i(n)$

$$\psi_m(n)=2^{(N-j)/2}\psi_i(2^{N-j}n). \tag{6}$$

Finally, we rewrite Eq. (1) as follows:

$$w(m,k)=2^{(N-j)/2}\sum_{n=0}^{L2^{j-1}}\bar{\psi}_i(2^{N-j}n-k)x(n), \tag{7}$$

where $n=t/\Delta t$, $L2^{j-1}$ denotes the length of the $\psi_m(n)$. Based on Eq. (7) the number of multiplication for the WT can be expressed as

$$MTL\sum_{j=1}^{N}2^{j-1}=MTL(2^N-1), \tag{8}$$

where $T$ denotes the length of the signal $x(t)$ (data length), $N$ the number of the analysis octaves, and $L$ the length of the $\psi_i(n)$ in $j=1$. As shown in Eq. (8), the amount of calculation in the conventional WT increases the exponentially as the analyzing octaves number $N$ increases, because the localization of $\psi_m(n)$ becomes bad as scale becomes large and the length $L2^{j-1}$ of $\psi_m(n)$ also increases exponentially. Moreover, the accuracy of computation becomes worse if the length of $\psi_m(n)$ is longer than the data length $T$, so the analysis minimum frequency (the maximum scale) will be limited by the length of the data for short data.

### 2.2. Basic fast algorithm of FWT

We can compute convolution in the frequency domain, for which we rewrite Eq. (1) as follows:

$$w(a,b)=a^{1/2}\int_{-\infty}^{\infty}\hat{x}(f)\bar{\hat{\psi}}(af)\mathrm{e}^{\mathrm{i}2\pi fb}\,\mathrm{d}f, \tag{9}$$

where $\hat{x}(f),\hat{\psi}(af)$ are Fourier transforms of the $x(t)$ and $\psi(t/a)$, respectively, and $\bar{\hat{\psi}}(af)$ denotes the complex conjugate of $\hat{\psi}(af)$. In addition a basic fast algorithm (BFA) of wavelet transform in the frequency domain has been developed [7].

As was done in Section 2.1, we first compute one octave of $\hat{\psi}_i(n)$ from $f_{\mathrm{N}}$, the minimum scale (analysis maximum frequency), $a=2^{i/M}\,(j=0)$,

$$\hat{\psi}_i(n)=2^{i/2M}\hat{\psi}(2^{i/M}n), \tag{10}$$

where $n = f/\Delta f$, and $\Delta f = 1/T$; $\Delta f$ denotes the frequency interval. We then use the self-similarity of the MW to obtain another MW for all octaves as follows:

$$\hat{\psi}_m(n) = 2^{j/2}\hat{\psi}_i(2^j n). \tag{11}$$

Consequently, the $\hat{x}(f)\bar{\hat{\psi}}(af)$ in Eq. (9) can be rewritten as follows:

$$w(m,n) = 2^{j/2}\hat{x}(n)\bar{\hat{\psi}}_i(2^j n). \tag{12}$$

So $W(m,k)$ which is a discrete expression of the $W(a,b)$ can be obtained by using the inverse Fourier transform about $k$ as follows:

$$w(m,k) = 2^{j/2}\sum_{n=0}^{T} w(m,n)\mathrm{e}^{\mathrm{i}2\pi(nk/T)}. \tag{13}$$

We now consider the number of multiplications for the BFA based on Eq. (13). Roughly, $L\log_2 L$ multiplications are required for one reverse Fourier transform and $T$ multiplications for $\hat{x}(n)$, and $\bar{\hat{\psi}}_m(n)$. That is, in order to calculate $W(m,k)$, we need the number of multiplications

$$MN(T + T\log_2 T) = MNT(1 + \log_2 T). \tag{14}$$

As shown above, the amount of calculation of FWT based on BFA is different from the WT, and is sensitive to the data length $T$. Moreover, the localization of the MW in the frequency domain becomes better as the scale becomes larger (analysis frequency becomes small). So the analysis range available in FWT will be larger than that in the conventional WT. Theoretically, the analyzable the frequency range of FWT is until when the length of $\psi_m(n)$ becomes one piece. For example, in this paper, FWT is analyzable to 10 octaves (4.9–5.0 kHz) with $T = 512$ and symmetrical boundary condition. However, the WT is analyzable only to six octaves (78 Hz–5.0 kHz) under the same conditions.

However, the FWT has a higher reconstructed error (RE) than that obtained by WT. In the following section, we will propose techniques to improve accuracy.

## 3. Examination of computation accuracy and speed

### 3.1. Improving accuracy

In order to compare the computational accuracy between WT and FWT, we used a model signal $x(t)$ shown in Fig. 1 along with its power spectrum. It has the property that each frequency component changes with time, and has 512 samples at a sampling frequency of 10 kHz. We use the RI-Spline wavelet which we proposed in [9] as the MW, and first perform a wavelet transform of the original signal $x(t)$ in order to get $W(a,b)$, then obtain the reconstructed signal $y(t)$ from the inverse wavelet transform. Fig. 2 shows the reconstructed error $|x(t) - y(t)|^2$ in dB, Fig. 2(a) shows the result obtained from the WT with 6 analysis octaves (78 Hz–5 kHz) and (b) shows the result obtained from the FWT based on the BFA with 10 analysis octaves (4.9 Hz–5 kHz). Both computations used 4 voices per octave.

It is clear by comparing Figs. 2(a) and (b) that the WT has a better performance than the FWT. In the case of the WT about $-40$ dB of RE has been obtained when removing the low frequency

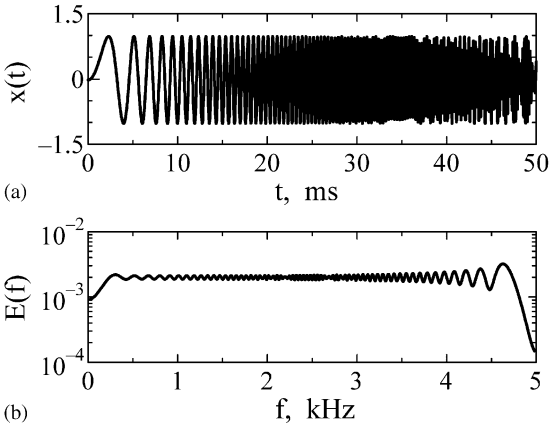


Fig. 1. (a) Model signal (b) Energy spectrum.

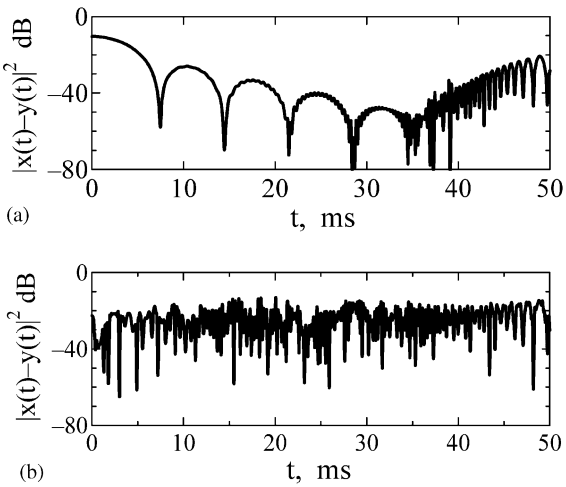


Fig. 2. RE by using WT and FWT based on BFA. (a) Reconstruction error by WT (b) Reconstruction error by FWT

domain and the high frequency domain, but in the case of the FWT only about −20 dB of RE has been obtained over the entire frequency domain. As shown in Section 2.2, all MWs in the case of the FWT based on the BFA are obtained from the MWs near the Nyquist frequency which have fewer data and calculation accuracy is low, although they have good localization in the time domain.

In order to improve the computational accuracy of the FWT, we use MWs whose frequencies are 2 octaves lower than the Nyquist frequency. This results in the corrected basic fast algorithm (CBFA). In this case, the length of the MWs in a time domain is extended 4 times from the length of the MWs near Nyquist frequency. If one fourth of the beginning of the data is used after carrying out the Fourier transform of the MWs with 4 times data length, the MWs obtained have the same length (localization) as the MWs near the Nyquist frequency. Fig. 3 shows the result obtained from the FWT using the CFBA. Fig. 3(a) shows the RE and (b) shows the basis system which was

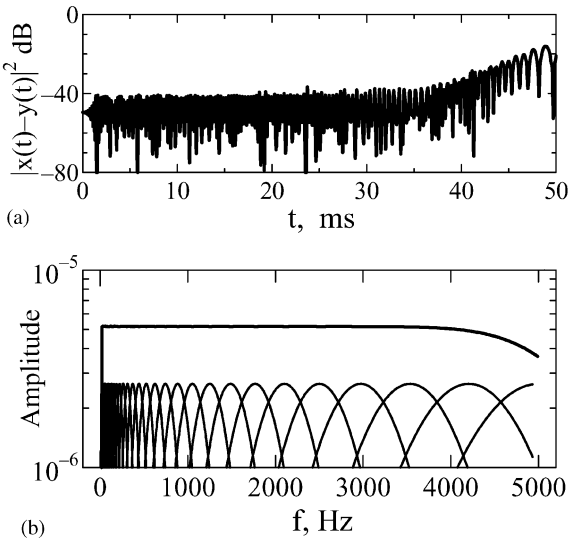


Fig. 3. RE improved by using FWT based on CBFA and wavelet bases for 10 octave, 4 divided. (a) Reconstruction error improved (b) Basis of FWT.

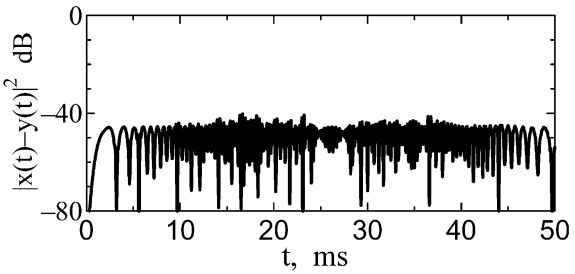


Fig. 4. RE by using FWTH.

constructed by $\hat{\psi}_m(n)$. As shown in Fig. 3, the FWT based on CBFA shows good performance. The RE obtained is lower than $-40$ dB over a wide frequency range and the accuracy is better than the result of WT shown in Fig. 2(a). Our method does not have any influence on the computational speed because the parameters in Eq. (14) have not been changed. However, in the high frequency domain, the problem that the RE is larger still remains. This is because when the frequency approaches $f_N$, the amplitude value of $\sum |\hat{\psi}(af)|/a$ (shown in Fig. 3(b)) becomes small.

In order to get a high degree of accuracy in the high frequency domain, we use up-sampling by using L-Spline interpolation. We assume that the sampling frequency is not changed after the data is interpolated although the number of samples increases twofold, so that the frequency of each frequency component falls by half. Therefore, the influence due to the reduction of the amplitude value of $\sum |\hat{\psi}(af)|/a$ near $f_N$ is avoided. This method is fast wavelet transform for high accuracy (FWTH). Fig. 4 shows the result obtained by using FWTH. As shown in Fig. 4, the RE obtained

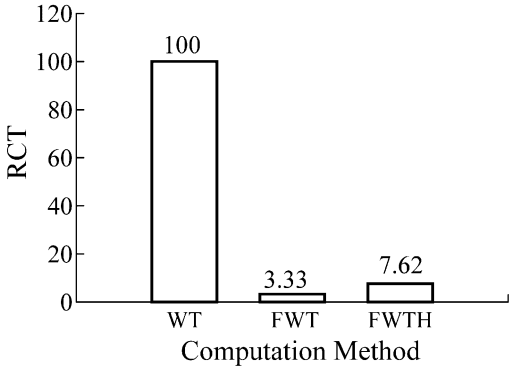


Fig. 5. Relative computation time (RCT).

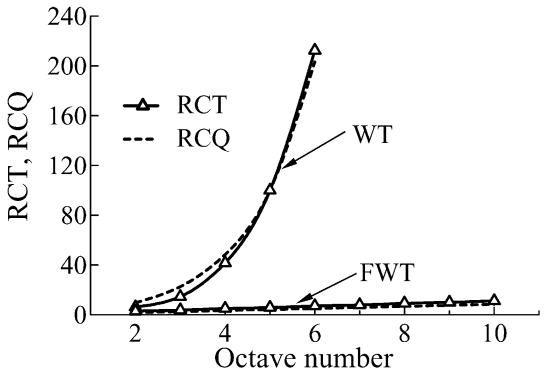


Fig. 6. RCT and RCQ change with octave number.

is lower than −40 dB over the entire frequency range. However, higher accuracy is as the expense of computational speed because the data length has been doubled.

### 3.2. Computational speed

The relative calculation time (RCT) for our methods is shown in Fig. 5. The analysis data length is 512, the number of analysis octaves is 6 and each octave has been divided to 4 voices. The RCT of each method is expressed relative to WT where calculation time is set at 100. As shown in Fig. 5, the computation time of FWT using CBFA is only 3.33. For FWTH, the computation time is only 7.62 although the data length is double in order to compute FWT with high accuracy. Based on the discussion above, we may conclude that the proposed fast wavelet transform is indeed effective for improving the computation accuracy at a high computation speed.

The RCT of FWT and WT changes with the increase in the number of analysis octaves was shown in Fig. 6. The ratio with computation quantity (RCQ) based on Eqs. (8) and (14) changes with the increase in the number of analysis octaves was also shown in Fig. 6 for comparison. The value of Both RCT and RCQ are expressed with the ratio that setting the value of WT in five

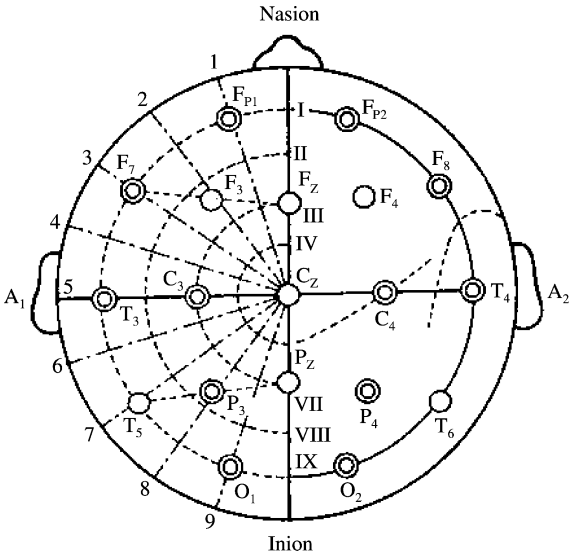


Fig. 7. Measured points of EEG.

octaves as 100. As shown in Fig. 6, the change of RCT about WT and FWT is well in agreement with RCQ. The calculation time of FWT increase is small, and oppositely, the calculation time of WT increases abruptly by the increase in the number of analysis octaves. This is well in agreement with the discussion in Section 2.2, and it is demostrated that the FWT can be adapted for a wider analysis frequency range than WT. Moreover, the change of RCT is the same as RCQ approximately with change of data length $T$ and voice number $M$, so RCT can be predicted using RCQ.

## 4. EEG analysis using FWT

EEG is an unsteady voltage signal of about 1–60 Hz and 5–300 μV at the suhace of the skull. The EEG frequency components around 2–4 Hz are usually defined as $\delta$ waves and the components around 4–8, 8–13 and 13–30 Hz as the $\theta, \alpha$, and $\beta$ waves, respectively. We will analyze the EEG using our FWT.

Fig. 7 shows arrangement of measurement electrodes of EEG. The marks, such as Fp1 in Fig. 7 are abbreviations of the electrode's location based on the ten-twenty electrode system. As shown in Fig. 7, Fz and Pz are placed on a straight line which connects the nasion and inion, C3 and C4 are placed on a straight line which connects both ear holes and the top of the head. Fig. 8 shows some EEGs of a 14-year-old girl recorded when she was sitting in a chair and opening her eyes. The data sampling frequency is 64 Hz so that the Nyquist frequency $f_N$ is 32 Hz. A spike and wave complex (SWC) around 3 Hz are recorded near 6–8, and 22–24 s.

In order to examine what was generated in SWC and what changed with time, we took out the parts of the SWC form EEG of FP2 in Fig. 8 and analyzed it by using the FWT. Fig. 9 shows the analysis results of SWC in FP2. Moreover, Fig. 9(a) is the result in 4–12 s and 9(b) is the result in 20–28 s, where the ordinates denote frequency, transverse time and the amplitude $|w(a,b)|$ is shown

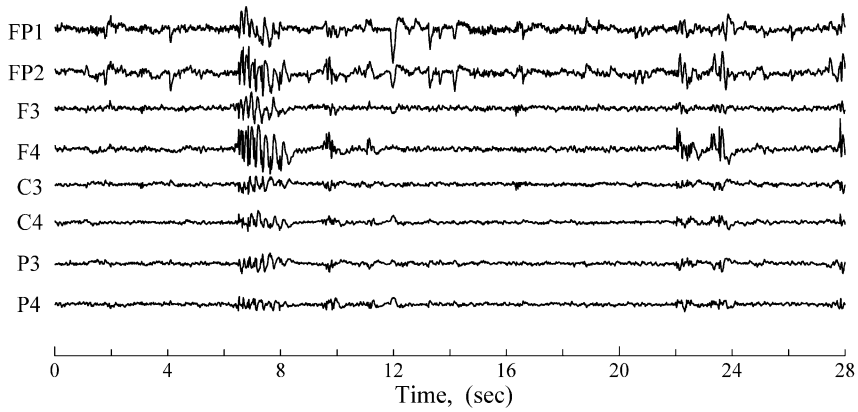


Fig. 8. Time series of EEG.

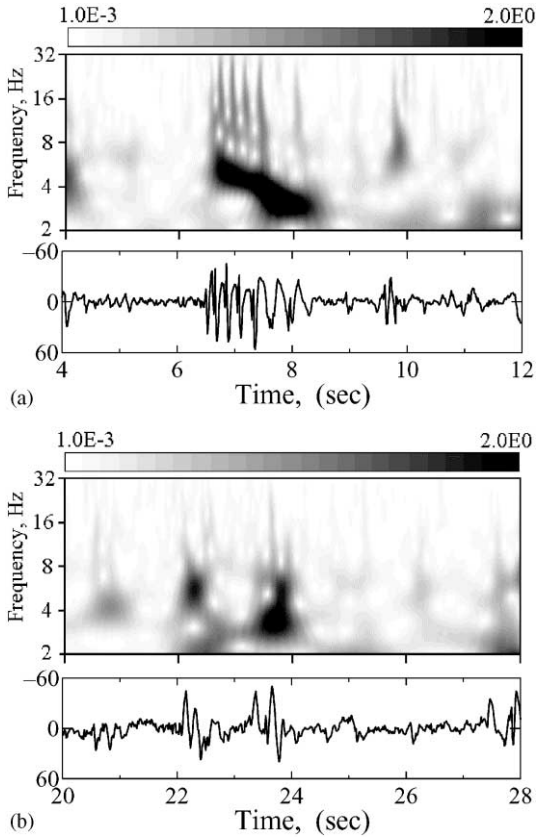


Fig. 9. Wavelet transform of EEG in point FP2. (a) Wavelet Transform of EEG in 4-12 sec (b) Wavelet Transform of EEG in 20-28 sec.

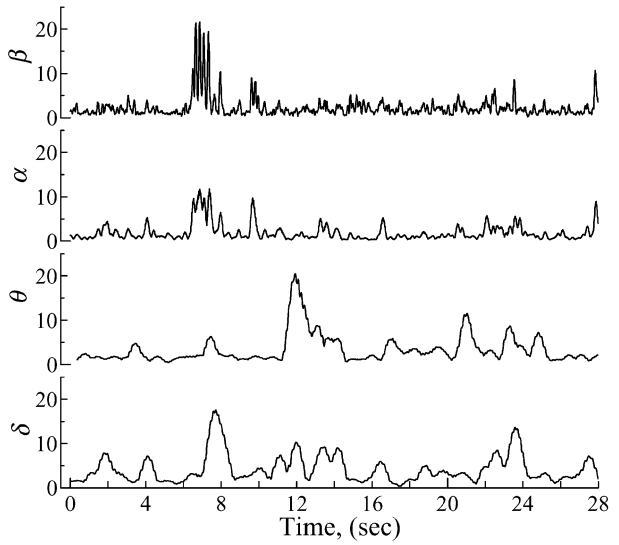


Fig. 10. RMS amplitude of $\delta$, $\theta$, $\alpha$ and $\beta$ wave of EEG in point FP2.

as the shade level. The analyzing frequency range was chosen as four octaves and each octave was divided into 48 voices for clarity. The computation time of FWT in above condition is about 17% of the traditional WT, the improvement of the computation efficiency is confirmed.

In Fig. 9(a) we can clearly see the $\alpha, \beta$, and $\theta$ waves near 6.4 s. The $\alpha$ and $\beta$ waves are intermittent. In contrast, the $\theta$ waves are continuous, but the frequency decreases with time, that is, the $\theta$ wave is changing to the $\beta$ wave with time. The $\alpha$ and $\beta$ waves were not observed between 22 and 24 s in Fig. 9(b), and the change of the $\theta$ wave is also intermittent. Moreover, the changes of SWC are different between that near 6–8 s and near 22–24 s although they are measured at the same point FP2 (Fig. 9).

In order to understand the process generating SWC, the $\delta$, $\theta, \alpha$, and $\beta$ waves were reconstructed from the wavelet transform of the EEG in FP2 shown in Fig. 8. Root mean square (RMS) amplitude are shown in Fig. 10. As is shown in Fig. 10, we can observe the active change of the $\delta, \theta, \alpha$, and $\beta$ waves before and after SWC occurred between 6 and 8 s. The same phenomenon was observed before and after SWC occurred between 22 and 24 s.

Moreover, the example of the RE of EEG by FWTH is shown in Fig. 11, and the RE of EEG by WT is also shown for comparison. As shown in Fig. 11, the accuracy obtained with FWTH is higher than WT. The average value of the RE of FWTH between 4 and 12 s is $-44$ dB and WT is 0.69 dB. Therefore, we may conclude that our approach proposed in this paper is effective for EEG analysis in real time with high accuracy.

## 5. Conclusion

In this paper, we propose a fast wavelet transform (FWT) which incorporates CBFA and FWTH to improve computation accuracy at a high computation speed. We examined the characteristics of FWT

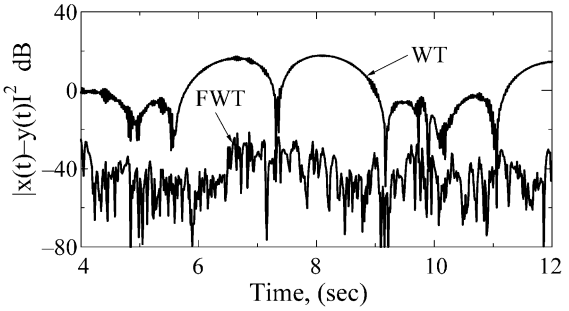


Fig. 11. RE of EEG in point FP2 from 4 to 12 s by using FWTH and WT.

using a model signal, and the experiments demonstrate advantages of our approaches. Furthermore, we used our method to analyze EEG; the results obtained show indeed they are effective. The main results obtained can be summarized as follows:

- For improving accuracy, we proposed the corrected basic fast algorithm (CBFA) that uses mother wavelets whose frequency is 2 octaves lower than the Nyquist frequency in the basic fast algorithm. FWT based on CBFA improved computation accuracy, at the same time realized high computation speed.
- Furthermore, to obtain a high degree of accuracy in the high frequency region, using up-sampling by the L-Spline interpolation, which we call fast wavelet transform for high accuracy (FWTH), is effective.
- Finally, the experimental results on the EEG data have shown that our method is effective for EEG analysis in real time with high accuracy and may be useful for other signal processing tasks.

## Acknowledgements

This work was supported in part by a grant (No.11680450) from the Ministry of Education, Science, Sports and Culture of Japan.

## References

[1] R. Sartene, L. Poupard, J.L. Bernard, J.C. Wallet, Sleep images using the wavelet transform to process polysomnographic signals, in: A. Aldroubi, M. Unser (Eds.), Wavelets in Medicine and Biology, CRC Press, Boca Raton, FL, 1996, pp. 355–382.
[2] S.J. Schiff, A. Aldroubi, M. Unser, S. Sato, Fast wavelet transform of EEG, Electroencephalogr and Clin. Neurophysiol. 91 (1994) 442–455.
[3] A. Aldroubi, The wavelet transform: a surfing guide, in: A. Aldroubi, M. Unser (Eds.), Wavelets in Medicine and Biology, CRC Press, Boca raton, FL, 1996, pp. 3–36.
[4] M. Unser, A practical guide to the implementation of the wavelet transform, in: A. Aldroubi, M. Unser (Eds.), Wavelets in Medicine and Biology, CRC Press, Boca Raton, FL, 1996, pp. 37–73.
[5] M.J. Shensa, The discrete wavelet transform: wedding the À Trous and Mallat algorithms, IEEE Trans. Signal Process. 40 (10) (1992) 2464–2482.

[6] M. Yamada, K. Ohkitani, An identification of energy casade in turbulence by orthonormal wavelet analysis, Prog. Theoret. Phys. 86-4 (1991) 799–815.
[7] M. Maeda, N. Yasui, H. Kitagawa, S. Horihata, An algorithm on fast wavelet transform/inverse transform and data compression for inverse wavelet transform, Proceedings of JSME 73rd General Meeting, No.96-1, pp.141–142 (in Japanese).
[8] O. Rioul, P. Duhamel, Fast algorithms for discrete and continuous wavelet transform, IEEE Trans. Inform. Theory 38 (2) (1992) 569–586.
[9] Z. Zhang, H. Kawabata, Unsteady signal analysis by using wavelet transform, Proceedings of the 1997 IEEE International Conference on Intelligent Processing Systems, pp. 1237–1241.

**Zhong Zhang** received his B.E. and M.E. degrees in 1982 and 1984, respectively, from Xi'an Highway University, China and his Ph.D. degree in 1993 from Okayama University, Japan. Dr. Zhang was a visiting scholar at the University of Melbourne, Australia in 1998. He is now a senior researcher at the Industrial Technology Center of Okayama Prefecture, and an Associate Professor at Okayama Prefectural University. His research and development interests include wavelet transform, neural networks and intelligent systems.

**Hiroaki Kawabata** received his B.E. degree in 1967 in Electrical Engineering and his Doctorate of Engineering degree in 1984, both from the University of Osaka Prefecture. Dr. Kawabata is a Professor at the School of Computer Scince and Systems Engineering of Okayama Prefectural University. He is engaged in research on neural networks and analysis of nonlinear systems.

**Zhi-Qiang Liu** received M.A.Sc. degree in Aerospace Engineering from the Institute for Aerospace Studies, The University of Toronto, and Ph.D. degree in Electrical Engineering from The University of Alberta, Canada. Dr. Liu is currently a Professor with School of Creative Media, City University of Hong Kong, and Department of Computer Science and Software Engineering, The University of Melbourne. He has taught Computer Architecture, Computer Networks, Artificial Intelligence, C programming language, Machine Learning, Pattern Recognition and computer graphics. His research and development interests include machine intelligence, fuzzy-neural systems, visual communications, biometric systems and applications, and web/data-mining. He also enjoys bush/beach walking, camping, classic music, and fishing—well, he has bought more fishing rods than the fish he caught.